

Magma emplacement process zone preserved in the roof of a large Cordilleran batholith, Wallowa Mountains, northeastern Oregon

Jiří Žák ^{a,*}, Kryštof Verner ^{b,c}, Kenneth Johnson ^d, Joshua J. Schwartz ^e

^a Institute of Geology and Paleontology, Faculty of Science, Charles University, Albertov 6, Prague, 12843, Czech Republic

^b Czech Geological Survey, Klárov 3, Prague, 11821, Czech Republic

^c Institute of Petrology and Structural Geology, Faculty of Science, Charles University, Albertov 6, Prague, 12843, Czech Republic

^d Department of Natural Sciences, University of Houston-Downtown, 1 Main Street, Houston, Texas, 77002, USA

^e Department of Geological Sciences, California State University Northridge, 18111 Nordhoff Street, Northridge, California, 91330, USA

ARTICLE INFO

Article history:

Received 20 October 2011

Accepted 2 March 2012

Available online 12 March 2012

Keywords:

Emplacement

Granite

Pluton roof

Process zone

Magmatic stoping

Wallowa batholith

ABSTRACT

The crestal portion of the upper-crustal Wallowa batholith, northeastern Oregon, provides an exceptional three-dimensional section through a flat batholith roof which rolls over into a steep wall at elevations of about 1600–2800 m. The roof–batholith margin is interpreted as representing the ‘frozen-in’ process zone of granodiorite magma which was arrested during its ascent, thus providing a direct view into processes that operate during construction of large, shallow-level Cordilleran-type batholiths. The batholith host rock records two principal and presumably coeval emplacement processes: ductile flow largely accommodated by rheologically weak and thus severely deformed marbles in the steep wall, and voluminous stoping of rheologically stronger, bedded siliciclastic rocks along the flat roof. Structures preserved along the roof suggest that the stoping was a multi-stage process involving emplacement of up to hundred meters long sills along bedding planes and formation of short connecting dikes cutting across bedding to produce sill–dike networks along the batholith–roof contact. Portions of the sill–dike networks and enclosed large rectangular roof blocks were then stoped into and continued to be mechanically disintegrated in the magma chamber. This inferred mechanism departs from the commonly assumed mode of stoped block formation solely by thermal shattering. In our view, host rocks in the process zone are fractured by dike propagation. It follows that such process of roof disruption and subsequent block stoping could be extremely rapid. In combination with other processes (e.g., roof uplift, ductile flow in weak lithologies), such rapid stoping could contribute to emplacement of voluminous and mostly non-sheeted Cordilleran-type batholiths at upper crustal levels.

© 2012 Elsevier B.V. All rights reserved.

1. Introduction

Pluton roofs provide the most rigorous insights into the emplacement processes of upper-crustal granitoid plutons and batholiths (e.g., Buddington, 1959; Cobbing and Pitcher, 1972; Myers, 1975; Paterson and Fowler, 1993a, b; Paterson et al., 1996; Paterson and Miller, 1998a, b; Yoshinobu et al., 2003; Rosenberg, 2004; Wagner et al., 2006; Žák and Paterson, 2006; Paterson and Farris, 2008; Grocott et al., 2009; Burchardt et al., 2010, 2012; Johnson et al., 2011a). Unfortunately, most plutons in the upper crust are exposed only in two-dimensional, approximately horizontal map sections, and the scarcity of direct field observations on pluton roofs is one of the main sources of controversies regarding pluton emplacement processes. Only mountainous areas with significant topography and difference in elevation of hundreds to thousands of meters can provide a more complete picture of the three-dimensional geometry of

their roofs and roof–wall transitions in order to better constrain emplacement mechanisms in the magma process zones, such as those previously described at dike tips (Rubin, 1995). It is in these regions that information is preserved on how host rock is displaced during rise/growth of magma bodies.

The purpose of this paper is to examine in detail the roof of the large, Cordilleran-type Early Cretaceous Wallowa batholith, Blue Mountains, northeastern Oregon (Figs. 1, 2). Both the roof and the underlying batholith are superbly exposed and reasonably accessible along a ridge with more than 1300 m of topographic relief (Fig. 2b), allowing direct observation and mapping of structures along the batholith/roof contact. Below we first briefly introduce the geologic setting of the Wallowa batholith and present pressure estimations from Al-in hornblende barometry to constrain its emplacement depth. We then describe in detail the three-dimensional geometry of the batholith roof and concentrate on mesoscopic structures along the batholith–roof contact. We also describe observations on xenoliths in the granodiorite–tonalite below the roof. Field observations, hornblende barometry, and structural data are then used as a background for general discussion on emplacement processes of

* Corresponding author.

E-mail address: jirizak@natur.cuni.cz (J. Žák).

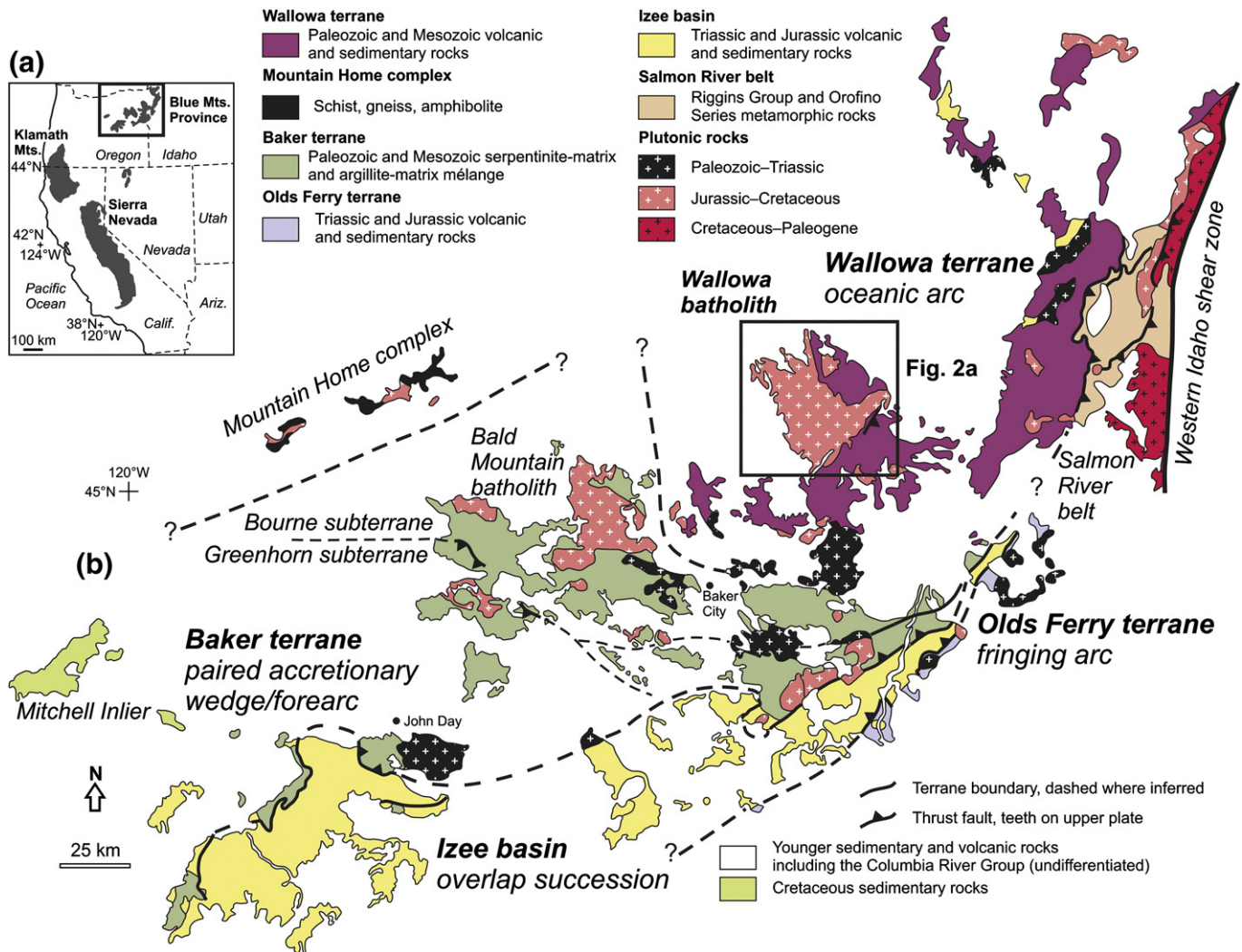


Fig. 1. (a) Map showing location of the Blue Mountains Province in the northwestern United States. Redrafted from Wyld et al. (1996). (b) Simplified geologic map showing terranes and their approximate boundaries in the Blue Mountains Province. The Wallowa batholith intrudes oceanic arc rocks of the most outboard Wallowa terrane. Redrafted from Schwartz et al. (2011a).

large-volume upper-crustal granitoid plutons and Cordilleran-type batholiths with a special emphasis on magmatic stoping and its role in the downward transport of host rock from collapsing roofs into magma chambers.

2. Geology of the Wallowa batholith: a brief overview

The Wallowa batholith is the largest (~620 km²) of multiple compositionally diverse plutonic bodies that intruded the Blue Mountains Province (Fig. 1b), an assemblage of amalgamated Permian to Jurassic oceanic arc terranes attached to the North American Craton during the Early Cretaceous (e.g., Thayer and Brown, 1964; Armstrong et al., 1977; Dickinson, 1979, 2004, 2008; Vallier and Brooks, 1995; Dorsey and LaMaskin, 2007; LaMaskin et al., 2009, 2011; Schwartz et al., 2011a, b and references therein). The batholith is composite and according to Taubeneck (1987) and Johnson et al. (2011b) consists of four main ~E–W trending plutons (from north to south; Fig. 2a): Pole Bridge pluton (140.2 ± 1.4 Ma), Hurricane Divide pluton (130.2 ± 1.0 Ma), Craig Mountain pluton (125.6 ± 0.6 Ma), and the Needle Point pluton (130.8 ± 1.5 Ma; Pb/U zircon ages after Johnson et al., 2011b). Overlapping ages and identical compositions of the ~130 Ma Hurricane Divide and Needle Point plutons (K. Johnson, unpublished data) suggest that they are virtually the same intrusion bifurcated by the youngest Craig Mountain pluton (Fig. 2a). Rocks

from the Pole Bridge, Hurricane Divide, and Needle Point plutons are compositionally extended from diorite to the most widespread amphibole–biotite granodiorite to tonalite with minor bodies of hornblende gabbro. These plutons are interpreted to be derived from a mantle source during the waning stages of Late Jurassic–Early Cretaceous arc activity associated with amalgamation of the Blue Mountains terranes (Johnson et al., 2011b). On the other hand, compositions of rocks of the Craig Mountain pluton are consistent with partial melting of thickened crust (Johnson et al., 2011b) following attachment of the Blue Mountains superterrane to the continental margin (dated at 128 ± 3 Ma by Getty et al., 1993). The last stage of Wallowa magmatism is represented by small satellite bodies of cordierite trondhjemite to the south of the main batholith (e.g., Taubeneck, 1964; Johnson et al., 1997, 2002).

The batholith is largely concealed by basalt flows of the Miocene Columbia River Group (Fig. 2a); intrusive contacts against the host rocks of the Wallowa oceanic arc terrane are exposed only along its northeastern and southeastern margins (Fig. 2a; Krauskopf, 1943). These volcanic and sedimentary arc-related rocks comprise here a ~300–460 m thick succession of Upper Triassic (Carnian–Norian) limestone and calcareous shales of the Martin Bridge Formation (Fig. 3a–e). These rocks were overlain conformably by Upper Triassic to Lower Jurassic (Norian–Sinemurian) bedded siliciclastic sedimentary rocks of the Hurwal Formation (Fig. 3a, f) comprising shales,

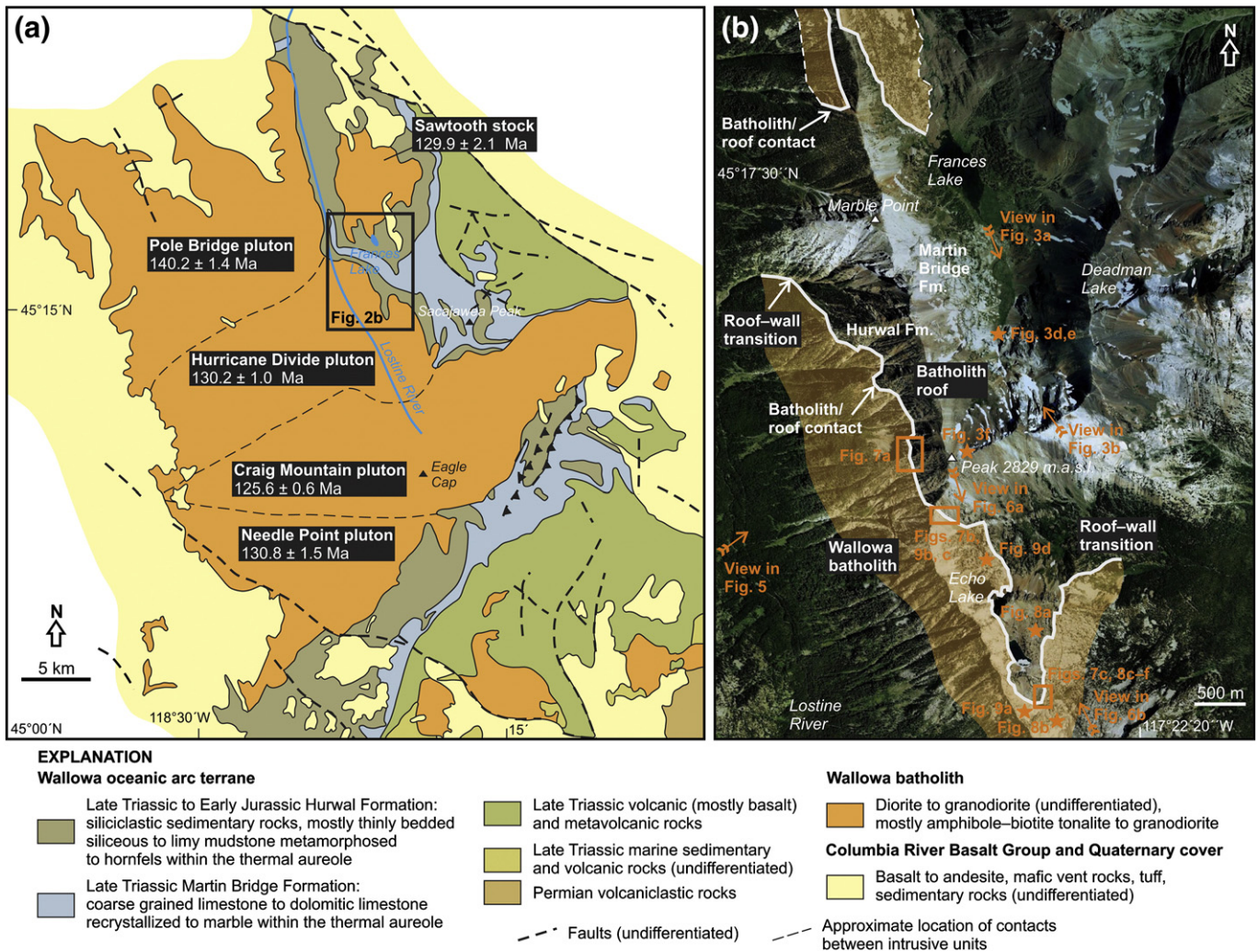


Fig. 2. (a) Simplified geologic map of the Wallowa batholith. The batholith is largely concealed beneath the Tertiary Columbia River Basalt Group. The southeastern contact dips moderately outwards according to Krauskopf (1943) whereas a large portion of the northeastern contact is an irregularly shaped pluton roof (this study). The batholith is composite and consists of four component intrusions emplaced over a time span of about 15 My. during the Early Cretaceous. This contribution examines the roof of the ~130 Ma Hurricane Divide pluton (outlined by bold rectangle). Geology compiled from Walker (1979) and Taubeneck (1987), radiometric ages taken from Johnson et al. (2011b). (b) Satellite image of the batholith roof exposed along a prominent ~NNE–SSW trending ridge above the Lostine River at elevations of about 2300–2500 m above the sea level. Stars indicate location of outcrop photographs presented in this paper, arrows indicate approximate direction of view from a distance. Background image taken from Google Maps.

siltstones, and quartzites of unknown total thickness (Smith and Allen, 1941; Weis et al., 1976; Stanley et al., 2008). Both successions have been affected heterogeneously by contact metamorphism and deformation which increase in intensity towards the batholith (Krauskopf, 1943). The contact metamorphic overprint produced a variety of hornfelsic rocks from siliciclastic protoliths but was most intense in the carbonate lithologies which are commonly recrystallized to marbles and calc-silicate rocks with tremolite, garnet, epidote, diopside, and wollastonite (Fig. 3d, e; Krauskopf, 1943). Away from the batholith, the degree of regional metamorphism is low in general and does not exceed greenschist-facies conditions.

3. Al-in hornblende barometry and emplacement depth of the batholith

Since the seminal work of Buddington (1959), pluton emplacement depth has been recognized as one of the key factors controlling emplacement processes. To better constrain the emplacement depth of the Wallowa batholith and its component plutons, we used the Al-in-hornblende barometer of Anderson and Smith (1995), which accounts for the effects of oxygen fugacity and temperature. Equilibrium temperatures were estimated using the hornblende–plagioclase

thermometer of Holland and Blundy (1994). Only compositions from adjacent hornblende and plagioclase rims were used in the estimates. Our pressure calculations are based on 29 hornblende–plagioclase pairs from 5 samples; the results are summarized in Tab. 1. Rocks from the Wallowa batholith yielded a range of pressure estimates from 0.11 to 0.26 GPa. In general, the Needle Point pluton yielded the highest pressure estimates (0.26 GPa), whereas the Craig Mountain pluton provided lower estimates of 0.11 to 0.22 GPa. The Hurricane Divide pluton, examined in detail in this study, yielded a pressure of 0.16 ± 0.06 GPa (Table 1), which is the same as a pressure estimate of 0.16 ± 0.06 GPa determined for the nearby Cornucopia stock (Johnson et al., 1997). In summary, the Al-in hornblende barometry corroborates a shallow emplacement depth of the Wallowa batholith (<7 km).

4. Overall three-dimensional geometry of the batholith roof

The exposed batholith–host rock contact is curvilinear to highly irregular even on a regional scale and consists of individual segments with variable strike and dip (Fig. 2a). The southeastern segment of the contact strikes roughly NE–SW and dips ~30°–60° outwards according to mapping by Krauskopf (1943) whereas the northeastern

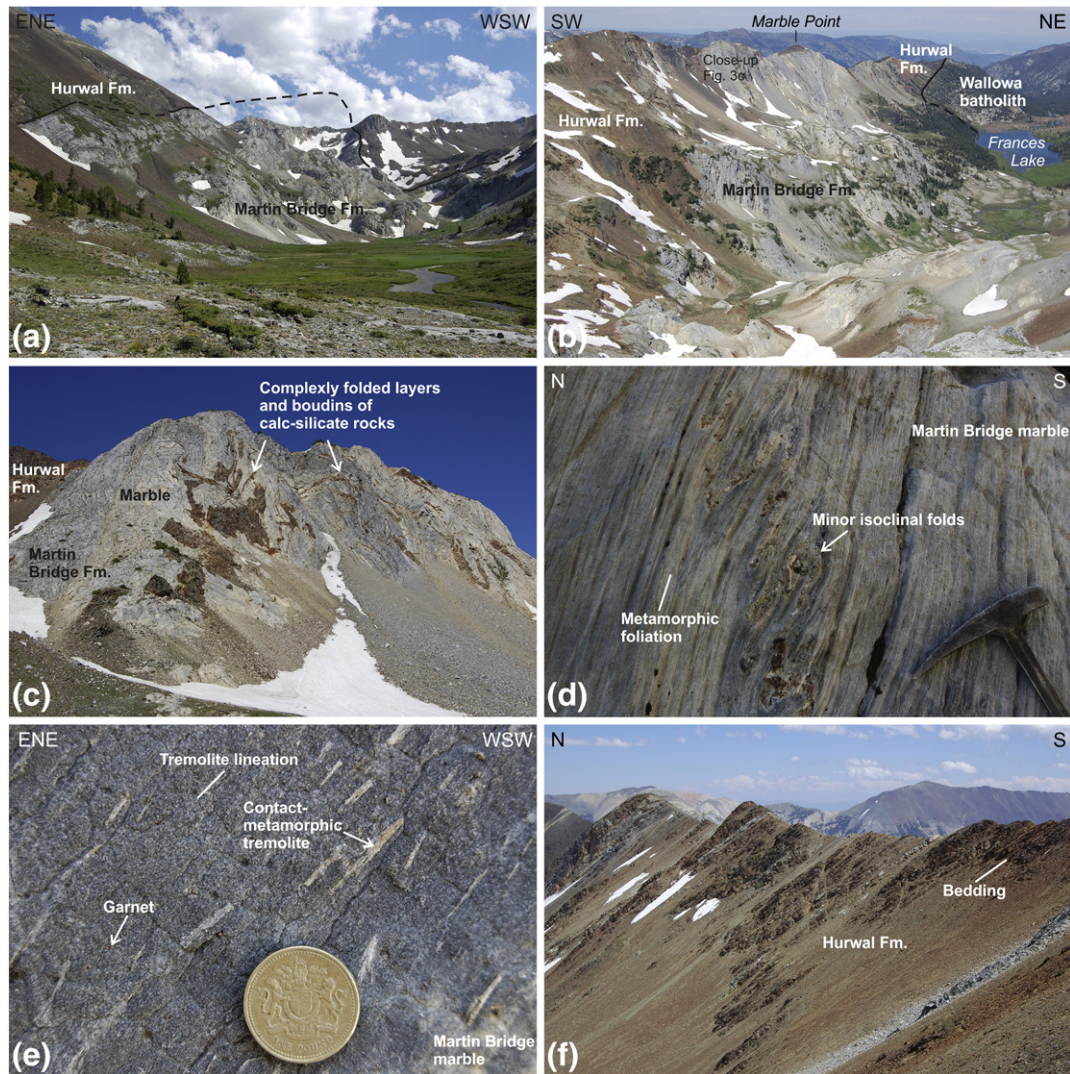


Fig. 3. Lithologic units and structures in the Wallowa batholith roof. (a) Folded anticlinal concordant contact between marbles of the Martin Bridge Formation and overlying siliciclastic rocks of the Hurwal Formation; valley southeast of Frances Lake. (b) Distant view of the roof and batholith–roof contact above Frances Lake. (c) Distant view on marbles of the Martin Bridge Formation containing folded layers and boudins of calc-silicate rocks; east face of Marble Point ridge. (d) Close-up view of minor isoclinal folds with their axial planes parallel to metamorphic foliation in marble of the Martin Bridge Formation; 1.1 km southeast of Frances Lake. (e) Mineral lineation in marble of the Martin Bridge Formation. The lineation is defined by fibres of contact-metamorphic tremolite; 1.1 km southeast of Frances Lake. (f) Monoclinical bedding in the siliciclastic rocks of the Hurwal Formation dipping moderately to the northeast; ridge to the south of Frances Lake. See Fig. 2b for location of photographs.

segment is more or less straight and steep at lower elevations (Fig. 2a), perhaps representing a side wall of the batholith. At the highest exposed elevations above 2500 m above sea level, the contact becomes flat and reveals a considerably more complex geometry (Fig. 2b). This portion of the contact shows generally flat to gently dipping attitude while it occupies the highest structural position in the entire batholith. It is thus the batholith roof (Fig. 4) and is dealt with in detail hereafter. This flat roof forms two narrow, approximately 1 km long projections that extend northward and southward from the main roof (Fig. 4a). As these projections follow a prominent ridge above the Lostine River valley (Figs. 2b, 4a) and the contact with the underlying batholith is generally flat to gently dipping (Fig. 5), their shape reflects intersection of the roof with the present-day topography. However, both these erosional remnants of the flat roof pass continuously sideways into steeper segments of the contact (Figs. 2b, 4a, c and 5).

5. Structure of the batholith roof

The large-scale structure in the mapped portion of the roof is defined by a major ~NW–SE trending tight anticline, where the marbles

and calc-silicate rocks of the Martin Bridge Formation occupy the core and the overlying siliciclastic rocks of the Hurwal Formation are exposed in the limbs, and a significantly smaller syncline to northeast containing a folded marble layer inside the Hurwal Formation (Fig. 4a, c). Even in the absence of reliable way-up indicators, stratigraphic relations combined with the orientation of bedding in the Hurwal Formation establish that the southwestern limb of the major anticline has been overturned (Figs. 3a, 4a, c). Although the relationship between both formations is generally concordant, they exhibit remarkably contrasting patterns of deformation. The marbles have been thoroughly recrystallized and exhibit pervasive metamorphic foliation, compositional banding, and tight to isoclinal minor folds defined by folded calcite veins or quartzite and calc-silicate intercalations (Fig. 3c, d). Metamorphic foliation and banding in the marbles strikes ~E–W to ~NW–SE and dips moderately to steeply to the NE (Fig. 4a, b). Mineral lineation, defined by elongated or fibrous grains of calcite, tremolite (Fig. 3e), and epidote shows a great scatter but tends to plunge moderately to the NE (Fig. 4a, b). In contrast, bedding is well preserved and chiefly planar (not folded into minor folds) in the siliciclastic rocks of the Hurwal Formation (Fig. 3f). In the southwestern overturned limb of the anticline, the bedding strikes

Table 1

Average hornblende and plagioclase compositions used in the pressure estimates. Abbreviations: P.B., Pole Bridge pluton; H.D., Hurricane Divide pluton; C.M., Craig Mountain pluton; N.P., Needle Point pluton; n, number of hornblende–plagioclase pairs used in the pressure estimates; FeO*, Total iron as FeO.

Sample	W98-46A		W98-22A		W98-36 C		W98-43		W98-83	
Pluton	P.B.		H.D.		C.M.		C.M.		N.P.	
n	5		5		4		6		9	
	ave.	S.D.	ave.	S.D.	ave.	S.D.	ave.	S.D.	ave.	S.D.
Hornblende										
SiO ₂	48.86	0.64	47.78	0.37	49.28	0.94	47.57	0.47	46.62	0.77
TiO ₂	0.53	0.22	1.11	0.40	0.60	0.10	0.96	0.26	0.62	0.11
Al ₂ O ₃	5.48	0.42	6.53	0.44	5.26	0.75	7.17	0.22	7.52	0.44
FeO*	13.78	0.25	13.91	0.69	12.54	0.27	13.93	0.45	16.20	0.83
MgO	14.45	0.21	14.09	0.51	15.02	0.17	13.83	0.34	12.60	0.62
MnO	0.40	0.01	0.33	0.04	0.66	0.11	0.45	0.10	0.30	0.02
CaO	11.99	0.09	12.00	0.22	11.85	0.22	11.77	0.56	12.07	0.12
Na ₂ O	0.80	0.10	1.03	0.21	0.89	0.19	0.86	0.15	0.90	0.06
K ₂ O	0.42	0.09	0.50	0.04	0.33	0.06	0.35	0.07	0.62	0.06
F	0.00	0.00	0.00	0.00	0.00	0.00	0.00	0.00	0.00	0.00
Cl	0.02	0.01	0.08	0.04	0.02	0.01	0.04	0.02	0.04	0.02
Total	96.73	0.18	97.37	0.73	96.42	0.54	96.93	0.39	97.50	0.50
Plagioclase										
SiO ₂	61.34	0.74	60.39	0.74	62.95	1.80	56.56	0.62	59.53	0.89
Al ₂ O ₃	24.53	0.36	25.51	0.54	23.80	1.63	27.71	0.36	25.93	0.73
FeO*	0.19	0.03	0.21	0.04	0.25	0.12	0.27	0.04	0.25	0.06
CaO	5.29	0.40	5.92	0.42	4.26	1.72	8.80	0.33	6.60	0.75
Na ₂ O	8.47	0.37	8.02	0.28	8.86	0.97	6.18	0.22	7.61	0.36
K ₂ O	0.22	0.05	0.20	0.05	0.27	0.07	0.20	0.05	0.21	0.09
Total	100.03	0.47	100.24	0.55	100.40	1.06	99.71	0.29	100.12	0.68
T (°C)	690	26	739	22	687	43	732	26	728	22
P (GPa)	0.13	0.02	0.16	0.02	0.11	0.04	0.22	0.04	0.26	0.03

~E–W to ~WNW–ESE to ~NW–SE and dips moderately to steeply to the NNE (Fig. 4a, b). Mineral and stretching lineations are absent. In general, the foliation and bedding in both formations are sub-parallel to the axial plane of the major anticline. Most importantly, at the map scale, the flat-lying upper contact of the batholith is discordant with structures in the overlying rocks (Fig. 4a).

6. Emplacement-related structures along the batholith–roof contact

The batholith–roof contact is structurally rather complex at the scale of meters to tens of meters (Figs. 5–8). In detail, the flat portion of the roof, predominantly composed of bedded siliciclastic rocks of the Hurwal Formation (Figs. 2b, 4, 5, and 6), has been intruded by numerous meters-thick sheets of granodiorite. The intrusive sheets are both concordant and discordant, that is, parallel to or at a high angle to the bedding, and are thus hereinafter referred to as sills and dikes, respectively. The roof exposes a downward gradation from isolated sills away from the roof margin (i.e., structurally above) that extend several hundred meters along strike (Fig. 5b) to a network consisting of interconnected sills and dikes (Fig. 7a). The adjacent sills and dikes delineate roughly rectangular roof-rock blocks several meters to tens of meters across and thus exemplify the extensive fragmentation of the batholith roof (Figs. 5b, and 7a). In some places, only tens of meters long sills are preserved along the roof margin and no dikes extend from the main granodiorite mass upward into the roof (Fig. 7b). However, even in these cases the roof–granodiorite contact takes abrupt, nearly 90° steps that are discordant and sharply truncate bedding. On the other hand, some portions of the roof have been intruded only by steep dikes (Fig. 6a), and sills or interconnected sill–dike networks are absent. In one zone below the roof (several tens of meters wide), xenoliths are particularly abundant (e.g., Fig. 6b) ranging in size from tens of meters down to decimeters in length. This near-contact zone then passes downward to non-sheeted granodiorite, which is either poor

in xenoliths or contains only scattered, variably-sized xenoliths (Fig. 6b).

Steep segments of the roof contain abundant sills and dikes that define a zone, several tens of meters wide, of extensive host rock fragmentation along the roof margin (Fig. 7c). However, this zone passes rather abruptly sideways into the non-sheeted and xenolith-poor granodiorite that lacks any visible internal contacts (e.g., Fig. 6b). Only in a few places are volumetrically minor sheeted complexes found either inside or at a distance of several tens of meters from the roof (Fig. 8a, b, respectively). These complexes typically consist of multiple decimeter- to meter-thick sheets of variable texture and composition ranging from diorite through tonalite to aplite.

In detail, a variety of small-scale structures along the roof margin provides further information on the emplacement processes and their relative succession. Some metapelitic lithologies commonly contain thin veins of leucosome either parallel to metamorphic foliation and banding or intensely folded into minor tight folds with foliation-parallel axial planes (Fig. 8c). The leucosome veins alternate with refractory metapelitic layers devoid of leucosome and display minor ductile deformation. Leucosomes and metapelitic layers are all intruded by thin granodiorite sills that truncate the ductile structures along knife-sharp contacts (Fig. 8c). In other places, thin host rock screens have been ductilely shortened, as evidenced by tightly folded bedding with fold axial planes parallel to the sheet margins (Fig. 8d) or by bedding that wraps around the blunt sheet tips (Fig. 8e). In addition, some of the sheets exhibit rather complex internal structure and contain margin-parallel schlieren layering or more irregularly-shaped concentrations of hornblende and biotite (Fig. 8d). The internal contacts between adjacent sheets are commonly delineated by trains of ductilely deformed and disrupted xenoliths. In some cases, the sheets wrap around xenoliths; whereas, in other cases, sheets have knife-sharp margins that truncate host rock markers in xenoliths with little to no evidence of ductile deformation (Fig. 8f).

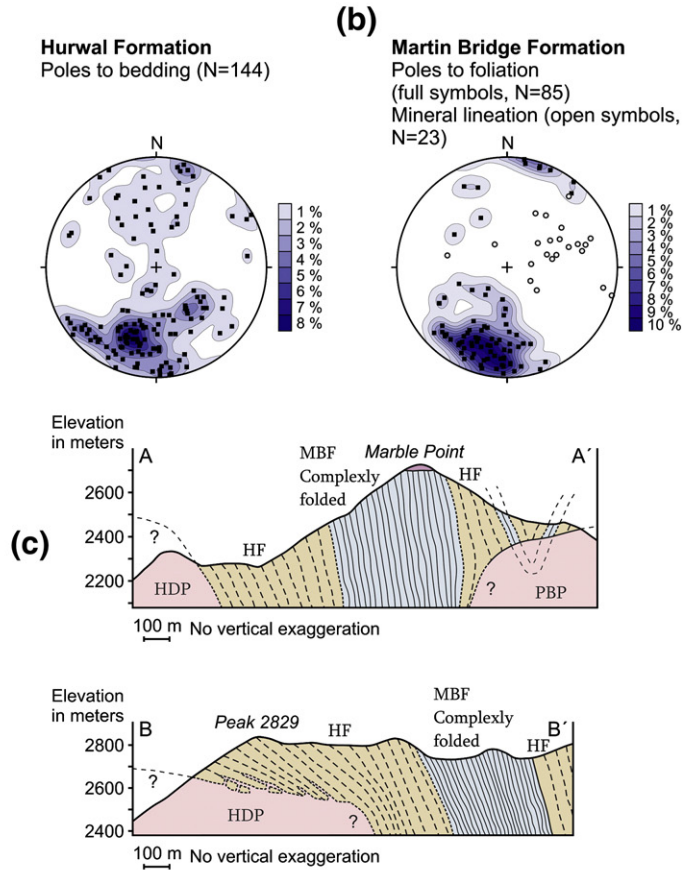
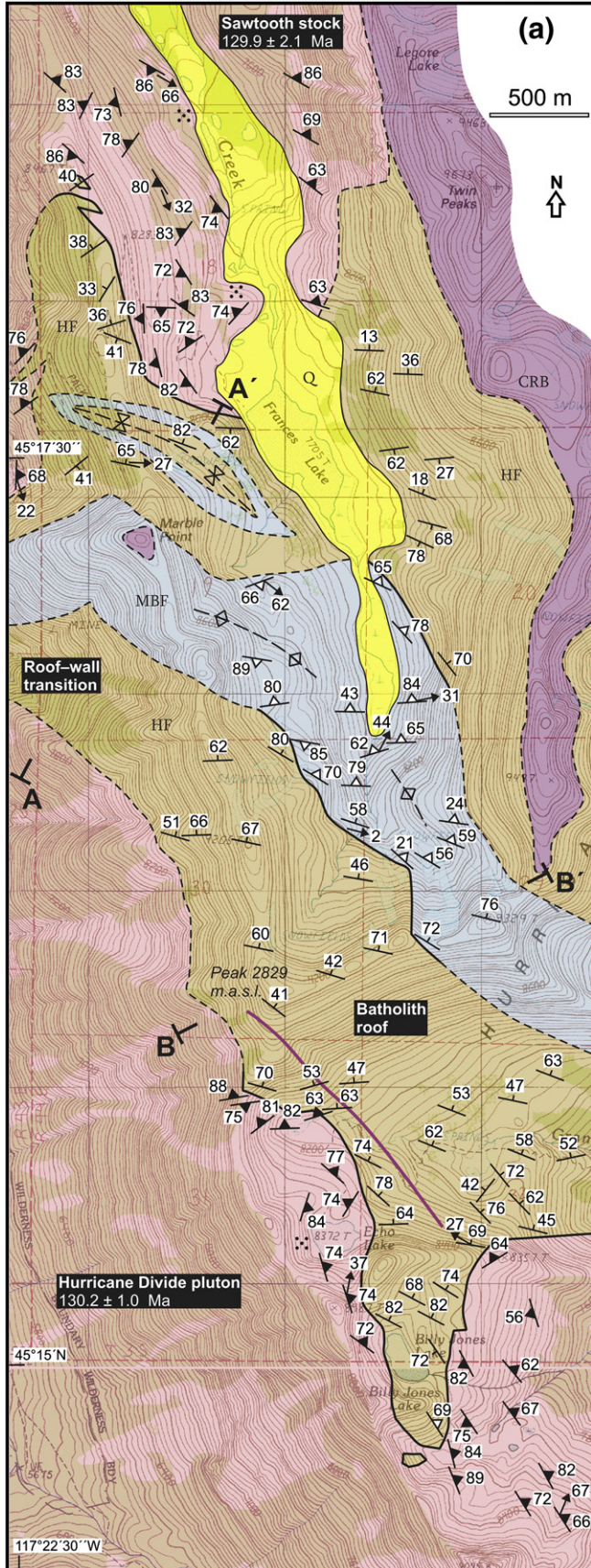
7. Xenoliths below the roof

As noted already by Krauskopf (1943), xenoliths are particularly abundant below some portions of the batholith roof (e.g., Fig. 7b) but may be entirely absent in other places. The vast majority of xenoliths in our study area are relatively compositionally uniform, dominated by siliciclastic rocks with various degree of contact metamorphic overprint and derived from the Hurwal Formation; carbonate and calc-silicate rocks correlative with the Martin Bridge Formation are rare. The sizes of xenoliths vary over several orders of magnitude from millimeters to tens of meters across. The largest xenoliths have typically rectangular shape (Fig. 9a) and are delimited by two contrasting types of outer margin. Margins that are discordant at a high angle to the strike of bedding in the xenoliths are irregular but simple and knife-sharp (Fig. 9b); whereas, margins concordant with bedding are commonly intruded by minor sills and disrupted into a mosaic of smaller blocks surrounded by the granodiorite (Fig. 9c). Reaction textures are rare along xenolith/host margins and are mostly limited to smaller (cm- to dm-sized) xenoliths. Inside, the xenoliths are either devoid of any intrusive sheets or commonly preserve the sill–dike network as normally seen in the near-contact zone of the batholith roof (compare Figs. 7a and 9a). Smaller xenoliths are rectangular to rounded and occur either isolated or in accumulations together with mafic microgranular enclaves (Fig. 9d). In some cases, the smaller xenoliths are aligned parallel to magmatic foliation in the host granodiorite.

It is important to note that xenoliths at greater distances from the roof commonly show the following evidence of their rotation and movement through the magma, suggesting that they are stopped blocks and not *in situ* rafts (see Paterson et al., 2008 for definitions and discussion): (1) Bedding inside these xenoliths exhibits multiple orientations that are remarkably different from the generally

monoclinical bedding attitude in the roof (e.g., Fig. 7b). (2) In some cases, the xenoliths are mingled with mafic microgranular enclaves. (3) Xenoliths are also aligned parallel to magmatic foliation in the

host granodiorite. (4) Away from the roof, xenoliths typically occur scattered in the non-sheeted, compositionally and texturally relatively uniform granodiorite with no internal contacts of any kind.



EXPLANATION	
Lithologic units	
	Quaternary cover (undifferentiated)
	Columbia River Basalt
	Wallowa batholith Granodiorite to tonalite, minor basic to intermediate rocks
	Hurwal Formation Siliciclastic sedimentary rocks, mostly thinly bedded siliceous to limy mudstone variably metamorphosed to hornfels
	Martin Bridge Formation Coarse-grained foliated marble with common quartzite boudins
Structural symbols	
	Strike and dip of bedding
	Strike and dip of metamorphic foliation
	Strike and dip of magmatic foliation
	No mesoscopic fabric apparent
	Trend and plunge of lineation
	Major anticline
	Major syncline
	Contact, certain (mapped)
	Contact, inferred or interpreted from afar (inaccessible)

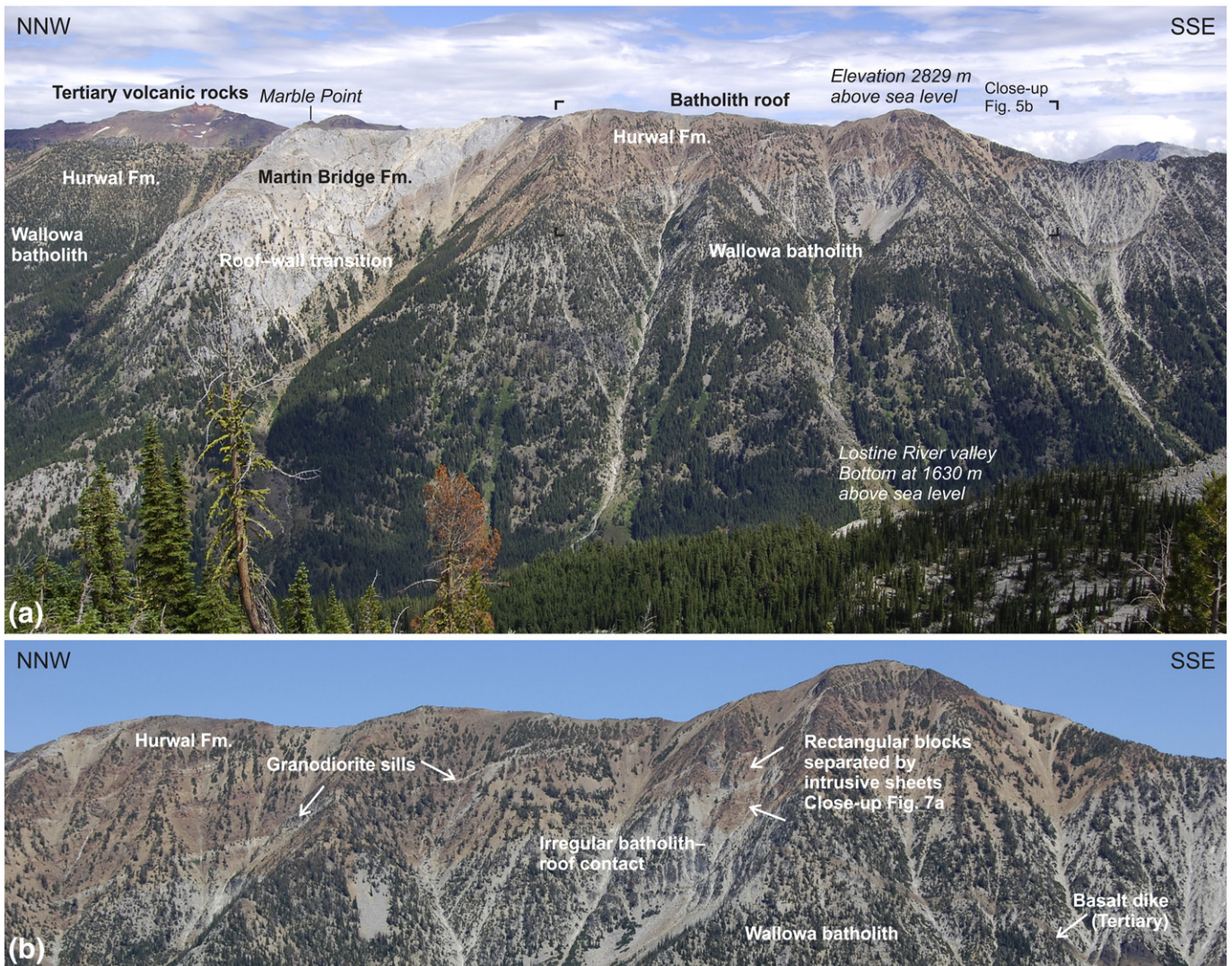


Fig. 5. Distant (a) and close-up (b) views of the Wallowa batholith roof exposed along a ridge above the Lostine River valley. The main portion of the batholith–roof contact dips gently but in detail the contact is highly irregular and disrupted by a network of intrusive sheets. See Fig. 2b for location of photographs.

8. Discussion

The traditional, long-held view of granitoid plutons as constructed episodically through only a single or a few large magma batches that can then persist in the crust as large long-lived chambers has been recently vigorously debated and challenged by the currently popular incremental growth hypothesis (for discussions see, e.g., Marsh, 1989, 2000; Coleman et al., 2004; Glazner et al., 2004; Morgan et al., 2004; Matzel et al., 2006; Miller et al., 2007; Bachmann and Bergantz, 2008a, b; Bartley et al., 2008; Burgess and Miller, 2008; Zellmer and Annen, 2008; Karlstrom et al., 2010; Memeti et al., 2010; Pignotta et al., 2010; Menand, 2011; Miller et al., 2011; an extensive discussion on this topic raged also on the granite-research listserv network in 2011). The latter hypothesis proposes that large volume plutonic bodies were never extensively molten at once but instead were constructed through numerous small magma additions (dikes or sills) that accumulated in a dike-by-dike manner (incrementally) to form a larger pluton. Thin dikes or sills should cool

rapidly below their solidi between injections implying that large magma reservoirs should be transient and rare features particularly in the cold upper crust. Were this hypothesis correct, some magma ascent mechanisms such as diapirism, voluminous stoping, or nested intrusion of large magma batches should not operate as commonly envisaged. However, the incremental growth hypothesis, although undoubtedly well applicable to some high-level laccoliths, smaller tabular plutons, and extensively sheeted complexes (e.g., Mahan et al., 2003; Walker et al., 2007; Michel et al., 2008; Farina et al., 2010; Horsman et al., 2010; Miller et al., 2011), faces serious difficulties to satisfactorily explain the emplacement of large vertically extensive and irregularly-shaped plutonic bodies. This hypothesis is also difficult to reconcile with the presence of large calderas and large-volume compositionally monotonous ignimbrites (monotonous intermediates) at the Earth's surface, requiring sizeable chambers of much larger volume than that of the erupted magma (e.g., Lipman, 1997, 2000, 2007; Bachmann et al., 2002, 2007; Jellinek and DePaolo, 2003; Bachmann and Bergantz, 2004; 2008a,b; Cole et al.,

Fig. 4. (a) Detailed geologic and structural map of the Wallowa batholith roof. Geology and structures are new mapping (this study), topographic background is trimmed USGS 7.5 Minute series maps, Chief Joseph Mountain and Eagle Cap quadrangles. (b) Stereonets (equal area, lower hemisphere projection) show orientation of bedding in the siliciclastic rocks of the Hurwal Formation and metamorphic foliation and associated mineral lineation in marbles of the Martin Bridge Formation. (c) Simplified interpretative cross-sections along lines A–A' and B–B' (location of lines is indicated in the map) across the roof of the Wallowa batholith. Dashed and solid lines within Hurwal and Martin Bridge units represent interpreted trace of bedding and metamorphic foliation, respectively.

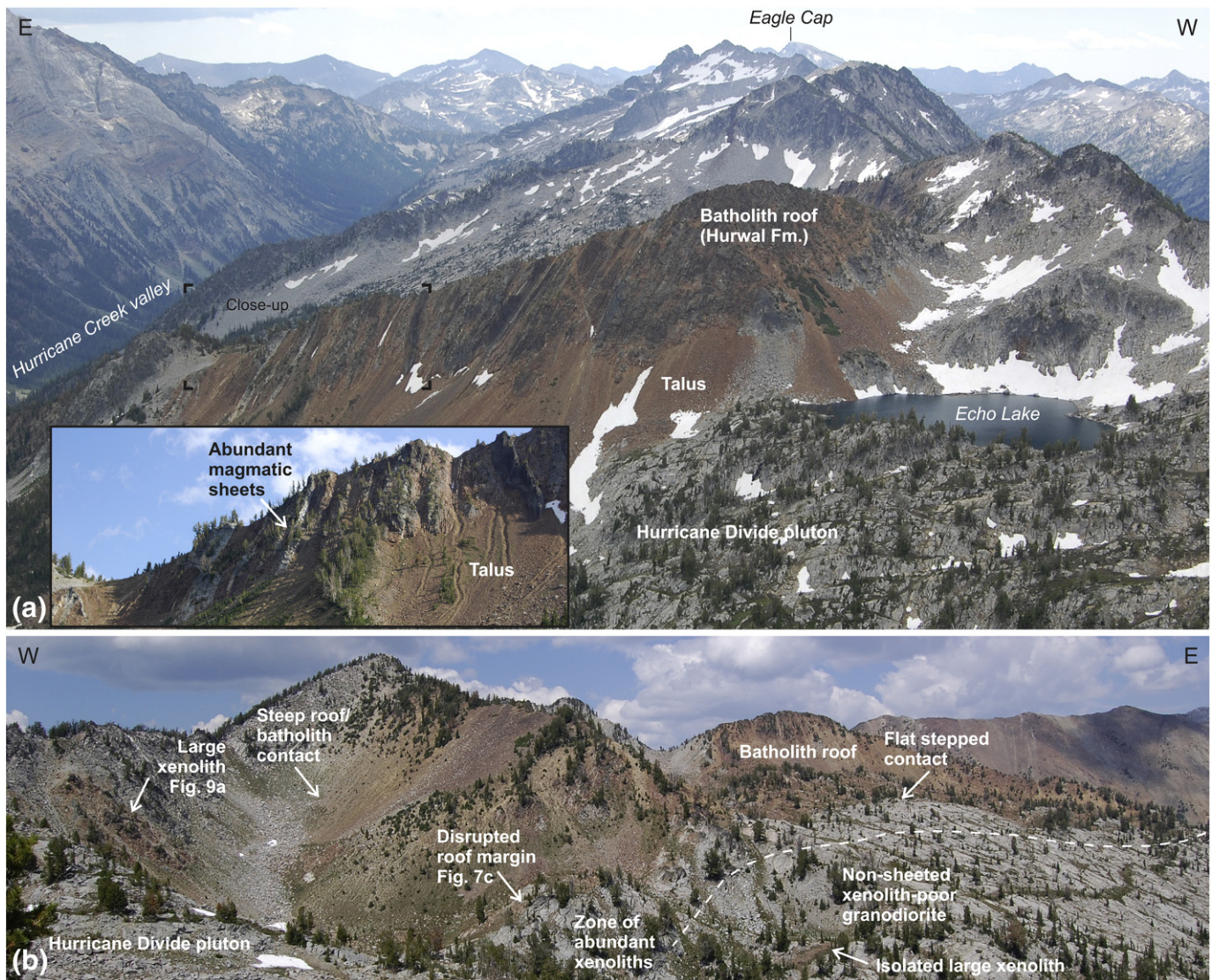


Fig. 6. Wallowa batholith roof to the southeast of Echo Lake. (a) Siliclastic sedimentary rocks of the Hurwal Formation in the roof intruded by subparallel steeply dipping intrusive sheets. (b) Irregular geometry of the batholith–roof contact consisting of steep and flat segments. View on the opposite (southern) side of the same ridge as shown in Fig. 6a. See Fig. 2b for location of photographs.

2005; Christiansen, 2005; de Silva and Gosnold, 2007; de Silva, 2008). One of the most common features of many plutons in continental-margin arcs and collisional orogens is the scarcity or even absence of internal contacts that must necessarily delineate the rapidly freezing magma increments, in particular at upper crustal levels (e.g., Vernon and Paterson, 2008; Žák et al., 2009; Hildebrand et al., 2010). This macroscopic homogeneity of plutons and their erupted equivalents is in many cases further complemented by their uniform geochemical characteristics over broad scales (for discussions see, e.g., Lipman et al., 1997; Bachmann and Bergantz, 2004; Metcalf, 2004; Bachmann et al., 2007; Lipman, 2007; de Silva and Gosnold, 2007; Bachmann and Bergantz, 2008a, b; Hildebrand et al., 2010; Fohey-Breting et al., 2011; Folkes et al., 2011) and by continuity and homogeneity in orientation of magmatic foliations and lineations across plutons (e.g., Paterson and Vernon, 1995; Žák et al., 2007; Bouchez, 2000). On a philosophical note, applying Occam's razor to this controversy, a more rational approach is to search for the potential mechanisms that could accommodate emplacement of relatively large magma batches of magma rather than applying incremental emplacement hypothesis to non-sheeted plutons that lack ubiquitous internal contacts.

8.1. Interpretation of the emplacement processes of the Hurricane Divide pluton

In light of our field observations and the above discussion, we believe that the Wallowa batholith roof preserves a frozen-in magma process zone that offers an exceptional view into the final emplacement of large-volume, Cordilleran-type plutons into the shallow crust (<7 km in this case according to Al-in-hornblende barometry). There are two striking features associated with the Wallowa batholith roof. First, contrasting styles of contact metamorphism and deformation were observed in the calc-silicate rocks of the Martin Bridge Formation and siliclastic rocks of the Hurwal Formation. The strong lineations defined by contact-metamorphic minerals (Fig. 3e) associated with pervasive foliation and tight to isoclinal folds (Fig. 3c, d) suggest intense syn-emplacement, ductile shortening in the calc-silicates as opposed to the monoclin, only moderately dipping and well-preserved bedding in the siliclastic rocks (Fig. 3f). Second, the flat portions of the roof are made up of the siliclastic rocks whereas the exposed steep pluton wall is predominantly composed of calc-silicate rocks (Fig. 5a). Our interpretation of the above is that the two contrasting patterns of deformation reflect two distinct but

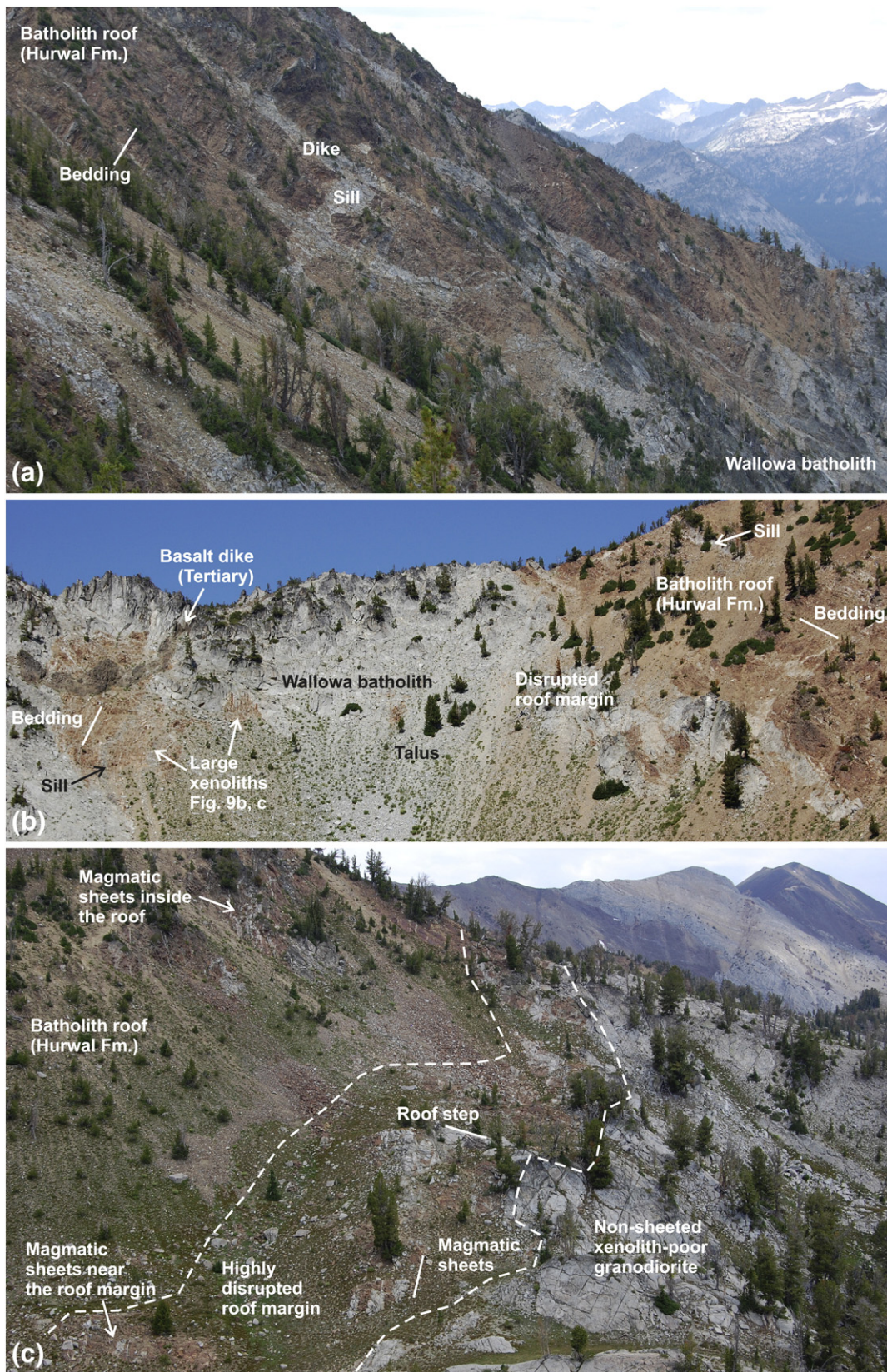


Fig. 7. Emplacement-related structures along the Wallowa batholith–roof contact. (a) Highly irregular roof margin disrupted by numerous concordant (bedding-parallel) and discordant (bedding-perpendicular) intrusive sheets that separate angular roof blocks tens of meters across. (b) Moderately dipping segment of the roof margin exhibiting stepped geometry and disrupted by bedding-parallel intrusive sheets in some places. Note the abundant irregularly shaped roof blocks inside the granodiorite. (c) Close-up of a steep segment of the roof margin (shown in Fig. 6b) extensively disrupted by intrusive sheets. See Fig. 2b for location of photographs.

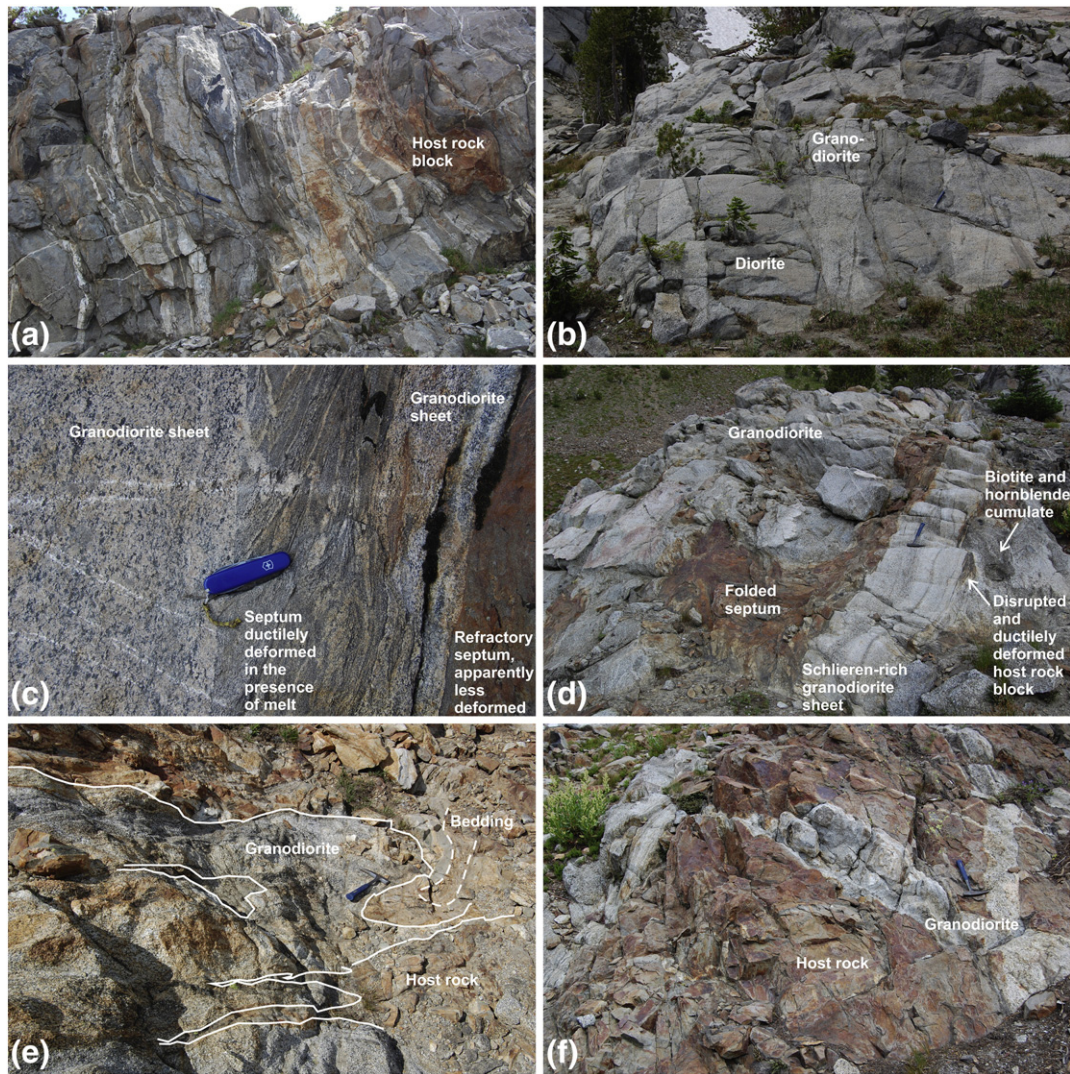


Fig. 8. Mesoscopic structures along the Wallowa batholith–roof contact. (a, b) Sheeted complexes inside and near the roof margin, respectively, consisting of amalgamated granodiorite and diorite sheets that enclose ductilely deformed and fractured host rock blocks. Hammer for scale. (c) Variably ductilely deformed screens of leucosome-bearing hornfelsic rocks intruded discordantly by granodiorite sheets. Swiss Army penknife (9 cm long) for scale. (d) Close-up of highly disrupted roof margin intruded by granodiorite sheets. The sheets are internally layered and bear abundant schlieren and concentrations of biotite and hornblende. The host rock screens have been ductilely deformed and dismembered during the sheet intrusion. Hammer for scale. (e) Blunt tips of intrusive sheets in the contact metamorphic siliciclastic rocks of the Hurwal Formation. Note that bedding is folded around some sheet tips. Hammer for scale. (f) Close-up of a network of granodiorite sheets oriented at a high angle to each other and separating angular blocks of metasedimentary host rock. Hammer for scale. See Fig. 2b for location of photographs.

broadly coeval rheologically controlled material transfer processes (MTPs of Paterson and Fowler, 1993a,b) accommodating emplacement of the Hurricane Divide pluton (Fig. 10). We suggest that the significantly weaker carbonates were capable of ductile flow at large scales even at the upper crustal level and were thus intensely shortened during magma emplacement (although some of the total strain could also be attributed to regional deformation; Figs. 3c, 10a). In contrast, the rheologically stronger, thinly bedded siliciclastic rocks deformed brittlely by fracture or by flexural slip at exactly the same emplacement level and thus presumably similar ambient temperature. These inferences are in concert with microstructural studies and experimentally determined flow laws indicating that marbles are rheologically weaker than quartz-dominated lithologies under most crustal conditions (e.g., Brodie and Rutter, 2000; Ulrich et al., 2002). Thus both ductile and brittle processes were operative simultaneously although in different lithologies and presumably at different rates during emplacement of a single pluton (e.g., Dietl, 1999; Miller and Paterson, 1999; Wang et al., 2000; Burov et al., 2003; Ciavarella and Wyld, 2008; Marko and Yoshinobu, 2011).

8.2. Mechanism of roof-rock stopping in the magma process zone

Structures preserved along the batholith–roof contact provide a detailed picture of how the brittle emplacement processes operated (Fig. 10b). We suggest that magma intruded first as approximately hundred meters long sills (Figs. 6a, b, and 10b) along the pre-existing planes of weakness as represented by bedding in the siliciclastic rocks. We see three possible mechanical explanations, or their combination, for the sill emplacement. First, the magma was driven passively into bedding planes that were parted as the roof rock differentially expanded owing to heating from the underlying magma (e.g., Clarke et al., 1998). Second, the sill emplacement was also passive, with the magma being drawn into bedding-parallel cracks, but the cracks opened in response to gravity-driven subsidence of the bedded roof rock into less dense magma (e.g., Clarke and Clarke, 1998). Third, the sills were emplaced forcefully by magma wedging (Hutton, 1992; Weinberg, 1999; Miller and Paterson, 2001). Implication of the latter would be that the magma was overpressured at the time of sill emplacement (e.g., due to

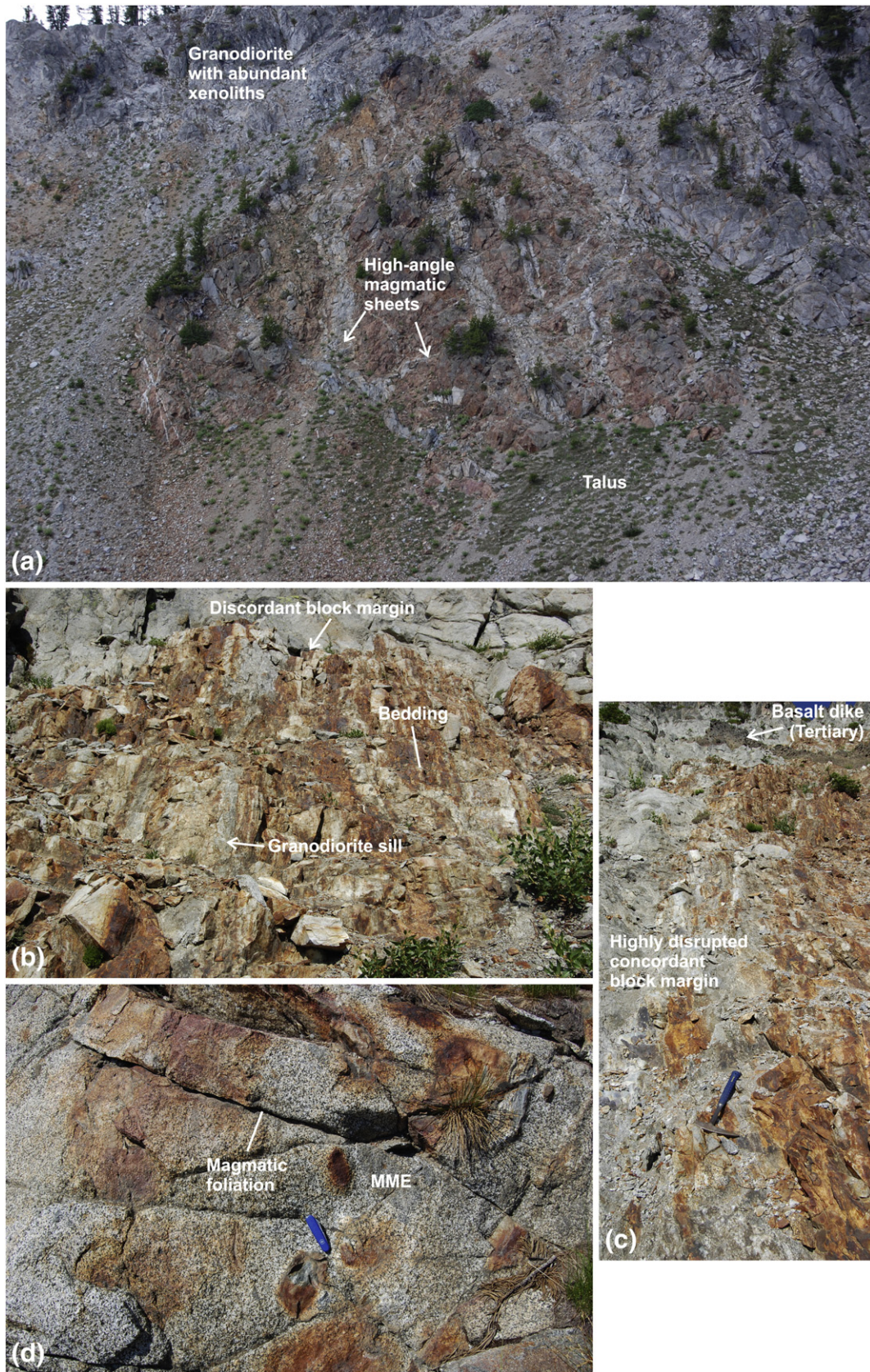


Fig. 9. Xenoliths in the Wallowa batholith. (a) A large xenolith (tens of meters across) of the siliciclastic rocks of the Hurwal Formation engulfed in the host granodiorite. The xenolith hosts a network of intrusive sheets that are at a high angle to each other. The granodiorite around the large block is littered with numerous smaller xenoliths. (b, c) Close-up views on contrasting, discordant and concordant xenolith margins. Hammer for scale. (d) Concentration of mafic microgranular enclaves (MME) and xenoliths of various size, shape, and composition. Some of the xenoliths are aligned parallel to magmatic foliation in the host granodiorite. Swiss Army penknife (9 cm long) for scale. See Fig. 2b for location of photographs.

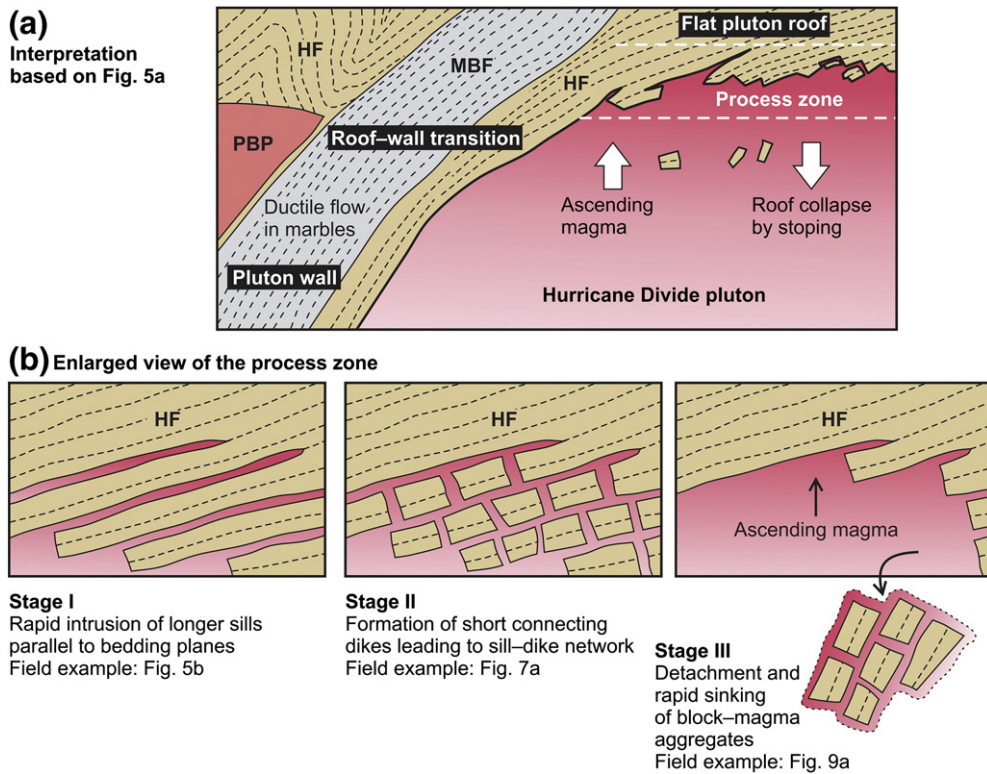


Fig. 10. Interpretative cartoon showing the ductile and brittle emplacement processes as inferred from our field observations in the Wallowa batholith and its host rock; see text for discussion. HF—Hurwal Formation, MBF—Martin Bridge Formation, PBP—Pole Bridge pluton.

buoyancy, tectonic stresses, and/or replenishment; Folch and Martí, 1998; McLeod and Tait, 1999; Jellinek and DePaolo, 2003). Subsequently, the thin roof-rock screens that separated the sills were intruded and fragmented by shorter connecting dikes that cut across the bedding (Fig. 10b). The connecting dikes may have utilized pre-existing joints (ubiquitous in shallow crust), formed as magma-driven self-propagating fractures (Clemens and Mawer, 1992), or accommodated gravity-driven brittle failure of the high-aspect-ratio inter-sill screens (continuum from the second process outlined above). In addition, dike emplacement was locally associated with ductile shortening and folding of wall rock (Fig. 8d, e).

Consequently, the emplacement of sills and dikes led to the development of an interconnected network of magma-filled cracks surrounding rectangular roof blocks tens of meters across (Figs. 6b, 7a, and 10b). Where not arrested by significantly diachronous cooling and solidification of the bounding intrusive sheets, we envision that adding magma to the fractured roof caused significant reduction of its overall strength (e.g., Hollister and Crawford, 1986; Pavlis, 1996; Zulauf and Helferich, 1997), a process that could potentially lead to a catastrophic, gravity-driven failure of pluton roofs and trigger volcanic eruptions (Hawkins and Wiebe, 2004). The aggregates of roof blocks enveloped by magma could have been then easily detached from the roof and stoped into the underlying magma chamber (Figs. 7b, 9a, and 10b). Once engulfed in the magma below the roof, some of the stoped blocks were intruded again by smaller sills and continued to mechanically disaggregate along the concordant margins (Fig. 9c).

Several recent studies suggested that, unlike the original view of stoping as a result of solely thermal cracking of the host rock (e.g., Daly, 1903; Marsh, 1982; Furlong and Myers, 1985), the removal of large blocks from the pluton roofs may also be a mechanical process facilitated by hydraulic fracturing of and dike emplacement into the roof (e.g., Pignotta and Paterson, 2007; Paterson et al., in press). Our inferences developed above support this latter view. Furthermore, several studies on dike transport of granitoid magmas have

postulated that the dikes may propagate rapidly in a crystal-poor low-viscosity state at rates as fast as $1 \text{ cm}\cdot\text{s}^{-1}$ to avoid freezing (Petford et al., 1993; Petford, 1996). If correct, the formation of sill-dike networks as described in this paper and the removal of blocks from the roof may also have been extremely rapid. After their entrapment into magma, large blocks may be rapidly transported downward since the rate at which blocks sink is much greater than the rate at which magmas crystallize (Marsh, 1982; Paterson and Miller, 1998a,b; Paterson and Okaya, 1999; Pignotta and Paterson, 2001; Pignotta and Paterson, 2007). For example, Marsh (1982) has demonstrated that a stoped block 10 m in size immersed in granitic magma will sink at a geologically instantaneous rate on the order of $\text{cm}\cdot\text{s}^{-1}$. At the exposed near-roof level through the Wallowa batholith, this assertion is supported by a general lack of reaction textures and by the presence of knife-sharp xenolith margins (e.g., Figs. 8d, f, and 10b), which favor rapid stoping with minor assimilation. Rapid removal and sinking of stoped blocks from the process zone is also supported by the narrow transition from the roof into underlying block-poor granodiorite (e.g., Figs. 6b, and 7c). We believe that the above proposed hypothesis has important implications for evaluating the efficacy of magma ascent by stoping in the crust. If the magma could extensively disrupt rigid roof rocks in the process zone by mechanical diking (a rapid process by definition regardless of the driving force), then its ascent by stoping through the upper crust may also be fast until the magma freezes by cooling from both the host rock and incorporated stoped blocks. In combination with other material transfer processes (e.g., ductile flow, roof uplift), this rapid process of stoping could contribute to emplacement of large portions of Cordilleran-type plutons and batholiths.

9. Conclusions

(1) The roof of the Wallowa batholith (specifically of the Hurricane Divide pluton), which is interpreted to represent the process zone of ascending magma, preserves a record of two main,

presumably coeval emplacement processes: ductile flow largely accommodated by rheologically weak and thus severely deformed marbles in the steep pluton wall, and voluminous stoping of strong, bedded siliciclastic rocks along the flat roof.

(2) Structures preserved along the roof suggest that the stoping was a multi-stage process involving emplacement of longer sills along bedding planes and formation of short connecting dikes cutting across bedding to produce sill–dike networks along the batholith–roof contact. Portions of the sill–dike networks surrounding large rectangular roof blocks were then stoped into and continued to be disintegrated in the magma chamber.

(3) This inferred mechanism departs from the commonly assumed mode of stoped block formation solely by thermal shattering of pluton roofs. It follows that if the host rock in front of the ascending magma path (i.e., in the process zone) is being disrupted mechanically by diking, the ascent of magma by stoping triggered by dike propagation could be rapid. In combination with other processes, it could effectively contribute to emplacement of voluminous and mostly non-sheeted Cordilleran-type batholiths at upper crustal levels.

Acknowledgements

We gratefully acknowledge Aaron Yoshinobu and Barrie Clarke for their highly detailed, thoughtful, and constructive reviews that led to significant improvement of the original manuscript. Mark Ferns is thanked for discussions, helping with maps, and taking care of our samples and field equipment. The first author (J.Ž.) also acknowledges Scott Paterson for discussions on pluton roofs and their significance for evaluating emplacement processes. The research was supported through a post-doctoral grant of the Grant Agency of the Czech Republic No. 205/07/P226 (to Jiří Žák) and from the Ministry of Education, Youth and Sports of the Czech Republic through Research Plan No. MSM0021620855. Partial financial support for this work was also provided by NSF grant EAR-0911681 (to Joshua Schwartz) and NSF grant EAR-0911735 (to Kenneth Johnson).

References

- Anderson, J.L., Smith, D.R., 1995. The effects of temperature and $f(\text{O}_2)$ on the Al-hornblende barometer. *American Mineralogist* 80, 549–559.
- Armstrong, R.L., Taubeneck, W.H., Hales, P.O., 1977. Rb–Sr and K–Ar geochronometry of Mesozoic granitic rocks and their Sr isotopic composition, Oregon, Washington, and Idaho. *Geological Society of America Bulletin* 88, 397–411.
- Bachmann, O., Bergantz, G., 2004. On the origin of crystal-poor rhyolites: extracted from batholithic crystal mushes. *Journal of Petrology* 45, 1565–1582.
- Bachmann, O., Bergantz, G., 2008a. The magma reservoirs that feed supereruptions. *Elements* 4, 17–21.
- Bachmann, O., Bergantz, G.W., 2008b. Rhyolites and their source mushes across tectonic settings. *Journal of Petrology* 49, 2277–2285.
- Bachmann, O., Dungan, M.A., Lipman, P.W., 2002. The Fish Canyon magma body, San Juan volcanic field, Colorado: rejuvenation and eruption of an upper-crustal batholith. *Journal of Petrology* 43, 1469–1503.
- Bachmann, O., Miller, C.F., de Silva, S.L., 2007. The volcanic–plutonic connection as a stage for understanding crustal magmatism. *Journal of Volcanology and Geothermal Research* 167, 1–23.
- Bartley, J.M., Coleman, D.S., Glazner, A.F., 2008. Incremental pluton emplacement by magmatic crack-seal. *Transactions of the Royal Society of Edinburgh: Earth Sciences* 97, 383–396.
- Bouchez, J.L., 2000. Anisotropie de susceptibilité magnétique et fabrique des granites. *Comptes Rendus Geoscience* 330, 1–14.
- Brodie, K., Rutter, E., 2000. Deformation mechanisms and rheology: why marble is weaker than quartzite. *Journal of the Geological Society, London* 157, 1093–1096.
- Buddington, A.F., 1959. Granite emplacement with special reference to North America. *Geological Society of America Bulletin* 70, 671–747.
- Burchardt, S., Tanner, D.C., Krumbholz, M., 2010. Mode of emplacement of the Slaufudalr pluton, southeast Iceland inferred from three-dimensional GPS mapping and model building. *Tectonophysics* 480, 232–240.
- Burchardt, S., Tanner, D.C., Krumbholz, M., 2012. The Slaufudalr pluton, southeast Iceland – an example of shallow magma emplacement by coupled cauldron subsidence and magmatic stoping. *Geological Society of America Bulletin* 124, 213–227.
- Burgess, S.D., Miller, J.S., 2008. Construction, solidification and internal differentiation of a large felsic arc pluton: Cathedral Peak granodiorite, Sierra Nevada Batholith. In: Annen, C., Zellmer, G.F. (Eds.), *Dynamics of crustal magma transfer, storage and differentiation*: Geological Society, London, Special Publications, 304, pp. 203–233.
- Burov, E., Jaupart, C., Guillou-Frottier, L., 2003. Ascent and emplacement of buoyant magma bodies in brittle-ductile upper crust. *Journal of Geophysical Research-Solid Earth* 108, 2177.
- Christiansen, E.H., 2005. Contrasting processes in silicic magma chambers: evidence from very large volume ignimbrites. *Geological Magazine* 142, 669–681.
- Ciavarella, V., Wyld, S.J., 2008. Wall rocks as recorders of multiple pluton emplacement mechanisms – examples from Cretaceous intrusions of northwest Nevada. In: Wright, J.E., Shervais, J.W. (Eds.), *Ophiolites, arcs, and batholiths: Geological Society of America Special Paper*, 438, pp. 517–550.
- Clarke, D.B., Clarke, G.K.C., 1998. Layered granodiorites at Chebucto Head, South Mountain batholith, Nova Scotia. *Journal of Structural Geology* 20, 1305–1324.
- Clarke, J.B., Henry, A.S., White, M.A., 1998. Exploding xenoliths and the absence of “elephants’ graveyards” in granite batholiths. *Journal of Structural Geology* 20, 1325–1343.
- Clemens, J.D., Mawer, C.K., 1992. Granitic magma transport by fracture propagation. *Tectonophysics* 204, 339–360.
- Cobbing, E.J., Pitcher, W.S., 1972. The Coastal Batholith of central Peru. *Journal of the Geological Society, London* 128, 421–460.
- Cole, J.W., Milner, D.M., Spinks, K.D., 2005. Calderas and caldera structures: a review. *Earth-Science Reviews* 69, 1–26.
- Coleman, D.S., Gray, W., Glazner, A.F., 2004. Rethinking the emplacement and evolution of zoned plutons: geochronologic evidence for incremental assembly of the Tuolumne Intrusive Suite, California. *Geology* 32, 433–436.
- Daly, R.A., 1903. The mechanics of igneous intrusion. *American Journal of Science* 15, 269–298.
- de Silva, S.L., 2008. Arc magmatism, calderas, and supervolcanoes. *Geology* 36, 671–672.
- de Silva, S.L., Gosnold, W.D., 2007. Episodic construction of batholiths: insights from the spatiotemporal development of an ignimbrite flare-up. *Journal of Volcanology and Geothermal Research* 167, 320–335.
- Dickinson, W.R., 1979. Mesozoic forearc basin in central Oregon. *Geology* 7, 166–170.
- Dickinson, W.R., 2004. Evolution of the North American Cordillera. *Annual Review of Earth and Planetary Sciences* 32, 13–45.
- Dickinson, W.R., 2008. Accretionary Mesozoic–Cenozoic expansion of the Cordilleran continental margin in California and adjacent Oregon. *Geosphere* 4, 329–353.
- Dietl, C., 1999. Emplacement of the Joshua Flat–Beer Creek Pluton (White Inyo Mountains, California): a story of multiple material transfer processes. In: Castro, A., Fernández, C., Vigneresse, J.L. (Eds.), *Understanding granites: integrating new and classical techniques*. Geological Society, London, Special Publications, 168, pp. 161–176.
- Dorsey, R.J., LaMaskin, T.A., 2007. Stratigraphic record of Triassic–Jurassic collisional tectonics in the Blue Mountains province, northeastern Oregon. *American Journal of Science* 307, 1167–1193.
- Farina, F., Dini, A., Innocenti, F., Rocchi, S., Westerman, D.S., 2010. Rapid incremental assembly of the Monte Capanne pluton (Elba Island, Tuscany) by downward stacking of magma sheets. *Geological Society of America Bulletin* 122, 1463–1479.
- Fohey-Bretting, N.K., Barth, A.P., Wooden, J.L., Mazdab, F.K., Carter, C.A., Schermer, E.R., 2011. Relationship of voluminous ignimbrites to continental arc plutons: petrology of Jurassic ignimbrites and contemporaneous plutons in southern California. *Journal of Volcanology and Geothermal Research* 189, 1–11.
- Folch, A., Martí, J., 1998. The generation of overpressure in felsic magma chambers by replenishment. *Earth and Planetary Science Letters* 163, 301–314.
- Folkes, C.B., de Silva, S.L., Wright, H.M., Cas, R.A.F., 2011. Geochemical homogeneity of a long-lived, large silicic system: evidence from the Cerro Galán caldera, NW Argentina. *Bulletin of Volcanology* 73, 1455–1486.
- Furlong, K.P., Myers, J.D., 1985. Thermal–mechanical modelling of the role of thermal stresses and stoping in magma contamination. *Journal of Volcanology and Geothermal Research* 24, 179–191.
- Getty, S.R., Selverstone, J., Wernicke, B.P., Jacobsen, S.B., Aliberti, E., 1993. Sm–Nd dating of multiple garnet growth events in an arc–continent collision zone, northwestern U.S. Cordillera. *Contributions to Mineralogy and Petrology* 115, 45–57.
- Glazner, A.F., Bartley, J.M., Coleman, D.S., Gray, W., Taylor, R.Z., 2004. Are plutons assembled over millions of years by amalgamation from small magma chambers? *GSA Today* 14, 4–11.
- Grocot, J., Arévalo, C., Welkner, D., Cruden, A., 2009. Fault-assisted vertical pluton growth: Coastal Cordillera, north Chilean Andes. *Journal of the Geological Society, London* 166, 295–301.
- Hawkins, D.P., Wiebe, R.A., 2004. Discrete stoping events in granite plutons: a signature of eruptions from silicic magma chambers? *Geology* 32, 1021–1024.
- Hildebrand, R.S., Hoffmann, P.F., Housh, T., Bowring, S.A., 2010. The nature of volcano–plutonic relations and the shapes of epizonal plutons of continental arcs as revealed in the Great Bear magmatic zone, northwestern Canada. *Geosphere* 6, 812–839.
- Holland, T., Blundy, J., 1994. Nonideal interactions in calcic amphiboles and their bearing on amphibole–plagioclase thermometry. *Contributions to Mineralogy and Petrology* 116, 433–447.
- Hollister, L.S., Crawford, M.L., 1986. Melt-enhanced deformation: a major tectonic process. *Geology* 14, 558–561.
- Horsman, E., Morgan, S., de Saint-Blanquat, M., Habert, G., Nugent, A., Hunter, R.A., Tikoff, B., 2010. Emplacement and assembly of shallow intrusions from multiple magma pulses, Henry Mountains, Utah. *Transactions of the Royal Society of Edinburgh: Earth Sciences* 100, 117–132.
- Hutton, D.H.W., 1992. Granite sheeted complexes: evidence for the dyking ascent mechanism. *Transactions of the Royal Society of Edinburgh: Earth Sciences* 83, 377–382.
- Jellinek, M., DePaolo, D.J., 2003. A model for the origin of large silicic magma chambers: precursors of caldera-forming eruptions. *Bulletin of Volcanology* 65, 363–381.

- Johnson, K., Barnes, C.G., Miller, C.A., 1997. Petrology, geochemistry, and genesis of high-Al tonalite and trondhjemites of the Cornucopia stock, Blue Mountains, northeastern Oregon. *Journal of Petrology* 38, 1585–1611.
- Johnson, K., Barnes, C.G., Browning, J.M., Karlsson, H.R., 2002. Petrology of iron-rich magmatic segregations associated with strongly peraluminous trondhjemite in the Cornucopia stock, northeastern Oregon. *Contributions to Mineralogy and Petrology* 142, 564–581.
- Johnson, S.E., Jin, Z.H., Naus-Thijssen, F.M.J., Koons, P.O., 2011a. Coupled deformation and metamorphism in the roof of a tabular midcrustal igneous complex. *Geological Society of America Bulletin* 123, 1016–1032.
- Johnson, K., Schwartz, J.J., Wooden, J.L., O'Driscoll, L.J., Jeffcoat, R.C., 2011b. The Wallowa batholith: new Pb/U (SHRIMP-RG) ages place constraints on arc magmatism and crustal thickening in the Blue Mountains Province, NE Oregon. *Geological Society of America Abstracts with Programs* 43, 5.
- Karlstrom, L., Dufek, J., Manga, M., 2010. Magma chamber stability in arc and continental crust. *Journal of Volcanology and Geothermal Research* 190, 249–270.
- Krauskopf, 1943. The Wallowa batholith. *American Journal of Science* 607–628.
- LaMaskin, T.A., Schwartz, J.J., Dorsey, R.J., Snoke, A.W., Johnson, K., Vervoort, J.D., 2009. Mesozoic sedimentation, magmatism, and tectonics in the Blue Mountains Province, northeastern Oregon. *Geological Society of America Field Guide* 15, 1–17.
- LaMaskin, T.A., Vervoort, J.D., Dorsey, R.J., Wright, J.E., 2011. Early Mesozoic paleogeography and tectonic evolution of the western United States: insights from detrital zircon U–Pb geochronology, Blue Mountains Province, northeastern Oregon. *Geological Society of America Bulletin* 123, 1939–1965.
- Lipman, P.W., 1997. Subsidence of ash-flow calderas: relation to caldera size and magma chamber geometry. *Bulletin of Volcanology* 59, 98–118.
- Lipman, P.W., 2000. Calderas. In: Sigurdsson, H., Houghton, B.F., McNutt, S.R., Rymer, H., Stix, J. (Eds.), *Encyclopedia of Volcanoes*. Academic Press, pp. 643–662.
- Lipman, P.W., 2007. Incremental assembly and prolonged consolidation of Cordilleran magma chambers: evidence from the Southern Rocky Mountain volcanic field. *Geosphere* 3, 42–70.
- Lipman, P., Dungan, M., Bachmann, O., 1997. Comagmatic granophyric granite in the Fish Canyon Tuff, Colorado: implications for magma-chamber processes during a large ash-flow eruption. *Geology* 25, 915–918.
- Mahan, K.H., Bartley, J.M., Coleman, D.S., Glazner, A.F., Carl, B.S., 2003. Sheeted intrusion of the synkinematic McDoyle pluton, Sierra Nevada, California. *Geological Society of America Bulletin* 115, 1570–1582.
- Marko, W.T., Yoshinobu, A.S., 2011. Using restored cross sections to evaluate magma emplacement, White Horse Mountains, Eastern Nevada, U.S.A. *Tectonophysics* 500, 98–111.
- Marsh, B.D., 1982. On the mechanics of diapirism, stoping, and zone melting. *American Journal of Science* 282, 808–855.
- Marsh, B.D., 1989. Magma chambers. *Annual Review of Earth and Planetary Sciences* 17, 439–474.
- Marsh, B.D., 2000. Magma chambers. In: Sigurdsson, H., Houghton, B.F., McNutt, S.R., Rymer, H., Stix, J. (Eds.), *Encyclopedia of Volcanoes*. Academic Press, pp. 191–206.
- Matzel, J.E.P., Bowring, S.A., Miller, R.B., 2006. Time scales of pluton construction at differing crustal levels: examples from the Mount Stuart and Tenpeck intrusions, North Cascades, Washington. *Geological Society of America Bulletin* 118, 1412–1430.
- McLeod, P., Tait, S., 1999. The growth of dykes from magma chambers. *Journal of Volcanology and Geothermal Research* 92, 231–245.
- Menand, T., 2011. Physical controls and depth of emplacement of igneous bodies: a review. *Tectonophysics* 500, 11–19.
- Memeti, V., Paterson, S.R., Matzel, J.E.P., Mundil, R., Okaya, D., 2010. Magmatic lobes as “snapshots” of magma chamber growth and evolution in large, composite batholiths: an example from the Tuolumne intrusion, Sierra Nevada, California. *Geological Society of America Bulletin* 122, 1912–1931.
- Metcalfe, R.V., 2004. Volcanic–plutonic links, plutons as magma chambers and crust–mantle interaction: a lithospheric scale view of magma systems. *Transactions of the Royal Society of Edinburgh: Earth Sciences* 95, 357–374.
- Michel, J., Baumgartner, L., Putlitz, B., Schaltegger, U., Ovtcharova, M., 2008. Incremental growth of the Patagonian Torres del Paine laccolith over 90 k.y. *Geology* 36, 459–462.
- Miller, R.B., Paterson, S.R., 1999. In defense of magmatic diapirs. *Journal of Structural Geology* 21, 1161–1173.
- Miller, R.B., Paterson, S.R., 2001. Construction of mid-crustal sheeted plutons: examples from the north Cascades, Washington. *Geological Society of America Bulletin* 113, 1423–1442.
- Miller, J.S., Matzel, J.E.P., Miller, C.F., Burgess, S.D., Miller, R.B., 2007. Zircon growth and recycling during the assembly of large, composite arc plutons. *Journal of Volcanology and Geothermal Research* 167, 282–299.
- Miller, C.F., Furbish, D.J., Walker, B.A., Claiborne, L.L., Koteas, G.C., Bleick, H.A., Miller, J.S., 2011. Growth of plutons by incremental emplacement of sheets in crystal-rich host: evidence from Miocene intrusions of the Colorado River region, Nevada, USA. *Tectonophysics* 500, 65–77.
- Morgan, D.J., Blake, S., Rogers, N.W., DeVivo, B., Rolandi, G., Macdonald, R., Hawkesworth, C.J., 2004. Time scales of crystal residence and magma chamber volume from modelling of diffusion profiles in phenocrysts: Vesuvius 1944. *Earth and Planetary Science Letters* 222, 933–946.
- Myers, J.S., 1975. Cauldron subsidence and fluidization: mechanisms of intrusion of the Coastal Batholith of Peru into its own volcanic ejecta. *Geological Society of America Bulletin* 86, 1209–1220.
- Paterson, S.R., Fowler, T.K., 1993a. Re-examining pluton emplacement processes. *Journal of Structural Geology* 15, 191–206.
- Paterson, S.R., Fowler, K.T., 1993b. Extensional pluton-emplacement models: do they work for large plutonic complexes? *Geology* 21, 781–784.
- Paterson, S.R., Vernon, R.H., 1995. Bursting the bubble of ballooning plutons: a return to nested diapirs emplaced by multiple processes. *Geological Society of America Bulletin* 107, 1356–1380.
- Paterson, S.R., Miller, R.B., 1998a. Stopped blocks in plutons: paleo-plumb bobs, viscometers, or chronometers? *Journal of Structural Geology* 20, 1261–1272.
- Paterson, S.R., Miller, R.B., 1998b. Magma emplacement during arc-perpendicular shortening: An example from the Cascades crystalline core, Washington. *Tectonics* 17, 571–586.
- Paterson, S.R., Okaya, D.A., 1999. Why don't we see more stopped blocks in plutons?: Results from thermal–mechanical modeling. *Eos, Transactions, American Geophysical Union* 80, 983.
- Paterson, S.R., Farris, D.W., 2008. Downward host rock transport and the formation of rim monoclines during the emplacement of Cordilleran batholiths. *Transactions of the Royal Society of Edinburgh: Earth Sciences* 97, 397–413.
- Paterson, S.R., Fowler, T.K., Miller, R.B., 1996. Pluton emplacement in arcs: a crustal-scale exchange process. *Transactions of the Royal Society of Edinburgh: Earth Sciences* 87, 115–123.
- Paterson, S.R., Pignotta, G.S., Farris, D.W., Memeti, V., Miller, R.B., Vernon, R.H., Žák, J., 2008. Is stoping a volumetrically significant pluton emplacement process?: Discussion. *Geological Society of America Bulletin* 120, 1075–1079.
- Paterson, S.R., Memeti, V., Pignotta, G.S., Erdmann, S., Žák, J., Chambers, J., Ianno, I., in press. Formation and transfer of stopped blocks into magma chambers: the high-temperature interplay between focused porous flow, cracking, channel flow, host-rock anisotropy, and regional deformation. *Geosphere*, doi:10.1130/GES00680.1.
- Pavlis, T.L., 1996. Fabric development in syn-tectonic intrusive sheets as a consequence of melt-dominated flow and thermal softening of the crust. *Tectonophysics* 253, 1–31.
- Petford, N., 1996. Dykes or diapirs? *Transactions of the Royal Society of Edinburgh: Earth Sciences* 87, 105–114.
- Petford, N., Kerr, R.C., Lister, J.R., 1993. Dike transport of granitoid magmas. *Geology* 21, 845–848.
- Pignotta, G.S., Paterson, S.R., 2001. The role of stoping in the evolution of magmatic systems: field and modeling constraints from plutons in the Sierra Nevada batholith, California. *Geological Society of America Abstracts with Programs* 33, 333.
- Pignotta, G.S., Paterson, S.R., 2007. Voluminous stoping in the Mitchell Peak Granodiorite, Sierra Nevada batholith. *The Canadian Mineralogist* 45, 87–106.
- Pignotta, G.S., Paterson, S.R., Coyne, C.C., Anderson, J.L., Onezime, J., 2010. Processes involved during incremental growth of the Jackass Lakes pluton, central Sierra Nevada batholith. *Geosphere* 6, 130–159.
- Rosenberg, C., 2004. Shear zones and magma ascent: a model based on a review of the Tertiary magmatism in the Alps. *Tectonics* 23, TC3002.
- Rubin, A.M., 1995. Propagation of magma-filled cracks. *Annual Review of Earth and Planetary Sciences* 23, 287–336.
- Schwartz, J.J., Snoke, A.W., Cordey, F., Johnson, K., Frost, C.D., Barnes, C.G., LaMaskin, T.A., Wooden, J.L., 2011a. Late Jurassic magmatism, metamorphism, and deformation in the Blue Mountains province, northeast Oregon. *Geological Society of America Bulletin* 123, 2083–2111.
- Schwartz, J.J., Johnson, K., Miranda, E.A., Wooden, J.L., 2011b. The generation of high Sr/Y plutons following Late Jurassic arc–arc collision, Blue Mountains province, NE Oregon. *Lithos* 126, 22–41.
- Smith, W.D.P., Allen, J.E., 1941. Geology and physiography of the northern Wallowa Mountains, Oregon. Oregon Department of Geology and Mineral Industries Bulletin 14, 1–125.
- Stanley, G.D., McRoberts, C.A., Whalen, M.T., 2008. Stratigraphy of the Triassic Martin Bridge Formation, Wallowa terrane: stratigraphy and depositional setting. In: Blodgett, R.B., Stanley, G.D. (Eds.), *The terrane puzzle: new perspectives on paleontology and stratigraphy from the North American Cordillera*: Geological Society of America Special Paper, 442, pp. 227–250.
- Taubeneck, W.H., 1964. Cornucopia stock, Wallowa Mountains, northeastern Oregon: field relationships. *Geological Society of America Bulletin* 75, 1093–1116.
- Taubeneck, W.H., 1987. The Wallowa Mountains, northeast Oregon. In: Hill, M.L. (Ed.), *Geological Society of America Centennial Field Guide – Cordilleran Section*: Geological Society of America, pp. 327–332.
- Thayer, T.P., Brown, C.E., 1964. Pre-Tertiary orogenic and plutonic intrusive activity in central and northeastern Oregon. *Geological Society of America Bulletin* 75, 1255–1262.
- Ulrich, S., Schulmann, K., Casey, M., 2002. Microstructural evolution and rheological behaviour of marbles deformed at different crustal levels. *Journal of Structural Geology* 24, 979–995.
- Vallier, T.L., Brooks, H.C. (Eds.), 1995. *Geology of the Blue Mountains region of Oregon, Idaho, and Washington: petrology and tectonic evolution of pre-Tertiary rocks of the Blue Mountains region*: U.S. Geological Survey Professional Paper 1438, pp. 1–540.
- Vernon, R.H., Paterson, S.R., 2008. How extensive are subsolidus grain-shape changes in cooling granites? *Lithos* 105, 42–50.
- Wagner, R., Rosenberg, C.L., Handy, M.R., Möbus, C., Alibert, M., 2006. Fracture-driven intrusion and upwelling of a mid-crustal pluton fed from a transpressive shear zone – the Rieserferner Pluton (Eastern Alps). *Geological Society of America Bulletin* 118, 219–237.
- Walker, G.W., 1979. Reconnaissance geologic map of the Oregon part of the Grangeville quadrangle, Baker, Union, Umatilla, and Wallowa Counties, Oregon, scale 1:250,000. U.S. Geological Survey miscellaneous investigations series map No. I-1116.
- Walker, B.A., Miller, C.F., Claiborne, L., Wooden, J.L., Miller, J.S., 2007. Geology and geochronology of the Spirit Mountain batholith, southern Nevada: implications for timescales and physical processes of batholith construction. *Journal of Volcanology and Geothermal Research* 167, 239–262.

- Wang, T., Wang, X., Li, W., 2000. Evaluation of multiple emplacement mechanisms: the Huichizi granite pluton, Qinling orogenic belt, central China. *Journal of Structural Geology* 22, 505–518.
- Weinberg, R.F., 1999. Mesoscale pervasive felsic magma migration: alternatives to dyking. *Lithos* 46, 393–410.
- Weis, P.L., Gualtieri, J.L., Cannon, W.F., Tucek, E.T., McMahan, A.B., Federspiel, F.E., 1976. Mineral resources of the Eagle Cap Wilderness and adjacent areas, Oregon. U.S. Geological Survey Bulletin 1388–E, pp. 9–22.
- Wyld, S.J., Quinn, M.J., Wright, J.E., 1996. Anomalous(?) Early Jurassic deformation in the western U.S. Cordillera. *Geology* 24, 1037–1040.
- Yoshinobu, A.S., Fowler, J., Kenneth, T., Paterson, S.R., Llambias, E., Tickyj, H., Sato, A.M., 2003. A view from the roof: magmatic stoping in the shallow crust, Chita pluton, Argentina. *Journal of Structural Geology* 25, 1037–1048.
- Žák, J., Paterson, S.R., 2006. Roof and walls of the Red Mountain Creek pluton, eastern Sierra Nevada, California (USA): implications for process zones during pluton emplacement. *Journal of Structural Geology* 28, 575–587.
- Žák, J., Paterson, S.R., Memeti, V., 2007. Four magmatic fabrics in the Tuolumne batholith, central Sierra Nevada, California (USA): implications for interpreting fabric patterns in plutons and evolution of magma chambers in the upper crust. *Geological Society of America Bulletin* 119, 184–201.
- Žák, J., Paterson, S.R., Janoušek, V., Kabele, P., 2009. The Mammoth Peak sheeted complex, Tuolumne batholith, Sierra Nevada, California: a record of initial growth or late thermal contraction in a magma chamber? *Contributions to Mineralogy and Petrology* 158, 447–470.
- Zellmer, G.F., Annen, C., 2008. An introduction to magma dynamics. In: Annen, C., Zellmer, G.F. (Eds.), *Dynamics of crustal magma transfer, storage and differentiation*: Geological Society, London, Special Publications, 304, pp. 1–13.
- Zulauf, G., Helfferich, S., 1997. Strain and strain rate in a synkinematic trondhjemitic dike: evidence for melt-induced strain softening during shearing (Bohemian Massif, Czech Republic). *Journal of Structural Geology* 19, 639–652.